Optimizing biased semiconductor superlattices for terahertz amplification

Xiaoli Lei, Dawei Wang, Zhaoxin Wu, and M. M. Dignam

Citation: Appl. Phys. Lett. **105**, 062112 (2014); doi: 10.1063/1.4892833
View online: http://dx.doi.org/10.1063/1.4892833
View Table of Contents: http://aip.scitation.org/toc/apl/105/6
Published by the American Institute of Physics

APPLIED PHYSICS LETTERS **105**, 062112 (2014)

Optimizing biased semiconductor superlattices for terahertz amplification

Xiaoli Lei,[1,2] Dawei Wang,[3] Zhaoxin Wu,[1,a)] and M. M. Dignam[4]
[1]*Key Laboratory for Physical Electronics and Devices of the Ministry of Education, Xi'an Jiaotong University, Xi'an 710049, China*
[2]*Xi'an University of Post and Telecommunications, Xi'an 710061, China*
[3]*Electronic Materials Research Laboratory–Key Laboratory of the Ministry of Education and International Center for Dielectric Research, Xi'an Jiaotong University, Xi'an 710049, China*
[4]*Department of Physics, Engineering Physics and Astronomy, Queen's University, Kingston, Ontario K7L 3N6, Canada*

(Received 6 June 2014; accepted 30 July 2014; published online 14 August 2014)

Over the past 15 yr or more, researchers have been trying to achieve gain for electromagnetic fields in the terahertz frequency region using biased semiconductor superlattices, but with little success. In this work, we employ our model of the excitonic states in biased GaAs/$Al_{0.3}Ga_{0.7}As$ semiconductor superlattices to find the optimal structures for amplification of terahertz radiation. In particular, we determine the optimum well width, barrier width, and bias field for terahertz fields with frequencies ranging from 1 to 4 terahertz. We find that gain coefficients on the order of 40 cm^{-1} should be achievable over most of this frequency range.
[http://dx.doi.org/10.1063/1.4892833]

The terahertz (THz) region of the electromagnetic spectrum, which has wavelengths ranging from 1 mm to 30 μm (300 gigahertz—10 terahertz), has been the focus of intense research over the past decade or more. There are a wide variety of potential applications for THz radiation, for instance, in airport passenger screening,[1] and in material science[2] where it is used in ultrafast spectroscopic studies of semiconductor nanostructures to investigate many-body interactions and the dynamics of transitions between internal excitonic states.[3–10] Most of these applications require compact, tunable THz sources as well as efficient detectors. Unfortunately, designing such sources has proven very difficult as the THz band lies between the realms of electronics and optics. Free electron lasers provide tunable THz radiation but are not compact;[11] Quantum Cascade lasers are compact, but are not very tunable.[12] Nonlinear interactions in an air plasma provide broadband THz radiation but are not compact and cannot easily be made narrow-band.[13]

For many years, researchers have postulated that biased semiconductor superlattices (BSSL) could be used as compact, tunable THz sources through stimulated emission between Wannier-Stark ladder (WSL) states.[14–19] When an electric field F_o is applied to a superlattice with period d, the electron and hole minibands are destroyed and replaced by the WSL states, which are localized about the different superlattice sites and have energies given by $E_n = E_0 + n\hbar\omega_B$, where n is an integer and $\omega_B = eFd/\hbar$ is the Bloch oscillation frequency.[20] Because the WSL states are equally spaced in energy and the transition dipoles between neighboring states are all equal, it has been shown that one cannot achieve THz gain using the non-interacting electron WSL states.[21,22] It has been shown theoretically[23] that the electron-phonon interaction breaks the transition symmetry and that THz gain should be possible. However, experimentally, the evidence for such gain has been inconclusive.[23–27] More recently, it was proposed that the breaking of the WSL transition symmetry due to the electron-hole Coulomb interaction in undoped, optically pumped BSSLs could be exploited to achieve THz gain. The gain arises from transitions between different *excitonic* WSL states,[15,28–30] and the tunability of the gain is provided by the applied *dc* bias.[27,31]

In Fig. 1, we plot the energies of nine different 1s excitonic WSL states as a function of the bias field; the size of symbols on the curves is proportional to the optical dipole element, Q_n, of each excitonic WSL level. In the absence of the electron-hole Coulomb interaction, all of the energy levels would be equally spaced. However, the interaction clearly modifies the spacing. In particular, note the large difference between the energy separation of the $n = 0$ state and the $n = +1$ and $n = -1$ states for $F > 5$ kV/cm. It is this difference that we exploit to obtain THz gain. As is seen in Fig. 1, the excitonic WSL energies deviate most significantly from the linear dependence on field at low fields strengths. Thus, if one wishes to achieve THz gain at low frequencies (<4 THz), it is critical that the properties of the BSSL are carefully calculated and optimized at these lower bias fields.

Achieving THz gain in such superlattices is a difficult task that requires careful design of the BSSL and proper choice of the optical pumping wavelength and has not been achieved to date. It is important to note that the energies and THz transition dipole moments between different excitonic WSL states are strongly affected by the well width, barrier width, and bias field of the BSSL.[15,28] However, while optimizing these parameters to find the best BSSL for THz is desirable, it is experimentally prohibitive with respect to both time and cost as it would require the fabrication and testing of a large number of BSSLs. Therefore, the development and application of a theoretical model that can determine the optimal BSSL structures for a given THz frequency is highly desirable as it would provide experimentalists with guidance

[a)]Electronic mail: zhaoxinwu@mail.xjtu.edu.cn

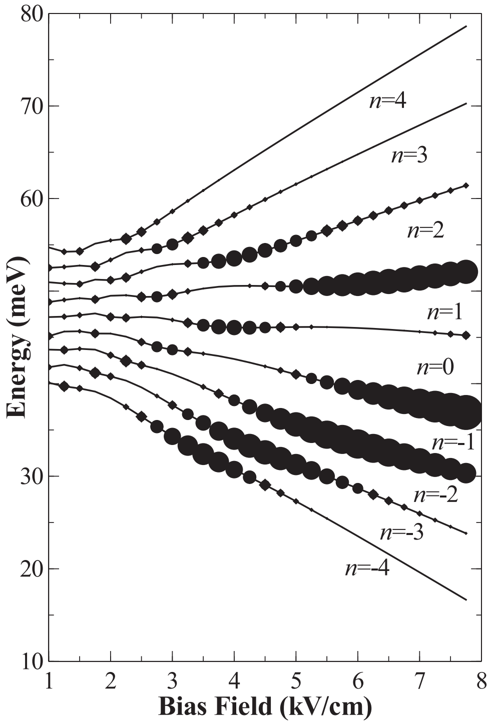

FIG. 1. The energy levels of the $1s$ excitons in the BSSL with barrier width, $b = 12$ Å and well width $w = 88$ Å as a function of the bias field when the electron-hole interaction is included. This structure is found to be optimal for the amplification of terahertz fields of central frequency $f = 2$ THz. The size of the symbols on each curve is proportional to the absolute value of the optical absorption coefficient, Q_n.

and specific design parameters to maximize the probability of success in observing and maximizing THz gain in BSSLs.

In this paper, we show that strong THz gain should be achievable in suitably designed, undoped, optically pumped $GaAs/Al_{0.3}Ga_{0.7}As$ BSSLs. The excitons are optically injected into the $n = 0$ $1s$ excitonic WSL state, and the structure is designed such that the energy difference between the $n = -1$ and $n = 0$ WSL levels is equal to the energy of the THz photons that are to be amplified (see Fig. 1). To achieve maximum gain, there are two main criteria: (i) the energy difference between the $n = 0$ and $n = +1$ WSL levels should be very different than the energy difference between the $n = -1$ and $n = 0$ WSL levels and (ii) the intraband dipole transition matrix element between the $n = 0$ and $n = -1$ WSL level should be large, while the element between $n = 0$ and $n = +1$ WSL levels be small. Note that the first of these criteria is clearly met for the BSSL of Fig. 1 for fields greater than about 5 kV/cm. Using these criteria and others, we design and implement a numerical algorithm to optimize the well width, barrier width, and bias field in the BSSL for THz gain at a given THz frequency between 1 and 4 THz. We find that the optimization results in gain coefficients greater than 40 cm^{-1} for most of this frequency range.

To model and optimize the gain in a BSSL, we employ a tight-binding model of $1s$ excitons in $GaAs/Al_{0.3}Ga_{0.7}As$ BSSLs that has been shown to give good agreement with experimental results for the excitonic WSL.[15,32,33] Here, we first present a brief summary of this approach. In the two-band envelope function approximation, the Hamiltonian for excitons in a superlattice under a bias field is given by[15,34]

$$H(z_e, z_h, r) = H_0(z_e, z_h, r) + U^e(z_e) + U^h(z_h) + eFz, \quad (1)$$

where $U^e(z_e)[U^h(z_h)]$ is the superlattice potential for the electron [hole],[34,35] H_0 contains the kinetic and Coulomb energy terms of the electron-hole pair. Here, z_e and z_h denote the z coordinates of the electron and hole, respectively, $z \equiv z_e - z_h$ and r denotes the electron-hole separation in the x, y (transverse) plane. The exciton envelope function ψ_n^q is expanded using an exciton Wannier function as

$$\psi_n^q(r, z_e, z_h) = \frac{1}{\sqrt{N}} \sum_m e^{iqmd} W_n(r, z_e - md, z_h - md), \quad (2)$$

where m is an integer, N is the number of lattice sites, q is the exciton wave number in the z direction, d is the periodicity of the BSSL under investigation, and $W_n(r, z_e, z_h)$ is the exciton Wannier function. The index n is a discrete quantum number of longitudinal motion that, in the high-field limit, gives the approximate separation of the electron and hole in units of the superlattice (SL) period and is thus approximately the WSL index described earlier. The WSL levels will be denoted by $n = 0, \pm 1, \pm 2, \ldots$ hereafter. Because we are interested in optically active excitons, we are only interested in the $q = 0$ states. The Wannier function $W_n(r, z_e, z_h)$ is calculated by expanding it in a basis of double well exciton wavefunctions where the expansion coefficients are obtained by diagonalizing the effective Hamiltonian.[15] In all that follows, we only consider the excitons that are $1s$-like in their in-plane motion, as it has been shown that these excitons dominate the optical and THz response when the system is optically excited on resonance with the $n = 0$ $1s$ WSL exciton state.[15] Using this formalism, the superlattice eigenstates, $|\psi_n^0\rangle$, and energies, $E_n = \hbar\omega_n$, can be obtained. Using the eigenstates, we calculate the terahertz dipole transition matrix elements along the superlattice axis, $G_{n,m} \equiv -e\langle\psi_n^0|\hat{Z}|\psi_m^0\rangle$, as well as the WSL optical absorption coefficients, Q_n. The material parameters used in our simulations can be found in Ref. 27.

After obtaining the properties of BSSLs, we use these to calculate the linear THz absorption gain coefficient by first calculating the linear susceptibility. We assume that the initial condition is that only the $n = 0$ excitonic WSL level is populated and that the THz field is a pure sinusoid. From standard quantum linear response theory,[36] the susceptibility arising from the excitons is given by

$$\chi(\omega) = \frac{e^2 N}{\epsilon_o} \sum_m \sum_{n>m} \frac{|G_{n,m}|^2 (p_m - p_n)}{\hbar(\omega_{nm} - \omega - i\Gamma_{nm})}, \quad (3)$$

where N is the 3D density of excitons and p_n is the probability of an exciton being in the nth state. The quantity, Γ_{nm}, is a phenomenological constant that is related to the full width at half maximum (Δ_{nm}) (FWHM) of the given transition by

$$\Delta_{nm} = \Gamma_{nm}/\pi. \quad (4)$$

We assume that experiment is performed at low temperatures (e.g., 10 K), that the $n = 0$ excitonic state is resonantly excited with a short (few hundred fs) optical pulse and that the THz pulse arrives within a few hundred femtoseconds after the optical pulse.[13] Because we will be considering

THz fields that are almost resonant at the Bloch frequency, ω_B, and initially only the $n=0$ WSL state is populated ($p_n=\delta_{n,0}$), we can assume that only the $n=-1, 0, +1$ states contribute significantly. We then obtain

$$\chi(\omega) \simeq \frac{e^2 N}{\epsilon_o}\left[-\frac{|G_{0,-1}|^2}{\hbar(\omega_- - \omega - i\Gamma)} + \frac{|G_{1,0}|^2}{\hbar(\omega_+ - \omega - i\Gamma)}\right], \quad (5)$$

where $\omega_+ \equiv \omega_{+1} - \omega_0$ and $\omega_- \equiv \omega_0 - \omega_{-1}$ are both positive quantities. For simplicity, we assume that the linewidths of both transitions are characterized by the single parameter, Γ. The complex wavenumber for the plane wave propagating through the medium is given by

$$k = k_o\sqrt{n_o^2 + \chi(\omega)}, \quad (6)$$

where n_o is the average index of refraction of the medium when the excitonic resonances are not included and $k_o \equiv \omega/c$. To obtain the absorption coefficients, we can write the wavenumber as

$$k = n(\omega)k_o + i\alpha(\omega)/2, \quad (7)$$

where $n(\omega)$ is the index of refraction and $\alpha(\omega)$ is the absorption coefficient[36]

$$\alpha(\omega) = \frac{\omega\chi''(\omega)}{cn_o}. \quad (8)$$

Combining Eqs. (5) and (8) and $\gamma(\omega) = -\alpha(\omega)$, we obtain the final expression for the gain coefficient (which is the negative of the absorption coefficient) at the THz frequency, f

$$\gamma(\omega) = \frac{e^2 N\hbar\omega\Gamma}{\hbar c n_o \epsilon_o}\left[\frac{|G_{0,-1}|^2}{(\hbar\omega_- - 2\pi\hbar f)^2 + (\hbar\Gamma)^2} - \frac{|G_{1,0}|^2}{(\hbar\omega_+ - 2\pi\hbar f)^2 + (\hbar\Gamma)^2}\right]. \quad (9)$$

This expression can now be used to optimize the BSSLs. For this purpose, we first calculated the excitonic states of a large number of BSSLs with well widths, w, between 10 Å and 98 Å, barrier widths, b, between 10 Å and 98 Å, and bias field, F, between 0 kV/cm and 30 kV/cm—resulting in a total of 245 025 data sets.[37] The selection process has two steps. First, we perform a preliminary screening to select only structures that meet the following criteria: (i) To ensure we are in the regime where the excitonic WSL states involved in the gain process resemble non-interacting WSL states, we require that the square of the optical absorption coefficients, Q_n, of the $n=0, \pm 1$ WSL levels together are larger than 40% of the sum over all WSL levels (i.e., $(|Q_{-1}|^2 + |Q_0|^2 + |Q_1|^2)/\sum_n Q_n^2 > 0.4$); (ii) We require that the absorption coefficient of the $n=0$ WSL level is not too small (i.e., $|Q_0/Q_{-1}| \geq 0.2$) because this is the WSL level the optical pulse excites; and (iii) We also require the $n=0$ to $n=-1$ intraband transition matrix element is large enough to provide strong intraband transitions ($|G_{0,-1}| > 0.04$ is used in practice). Then, after this initial screening, we compute the gain coefficient for each data set using Eq. (9). We assume that the experiments are run at a temperature close to 10 K and thus take the dephasing time to be 1.32 ps ($\hbar\Gamma = 0.5$ meV), which is chosen to be close to the value that has been found experimentally in a 67/17 BSSL at low temperature.[28,38] Finally, using the WKB approximation for the non-interacting electron and hole zero-field bands, we verified that the probability of Zerner tunneling out of the minibands of interest is negligible ($<10^{-3}$ per Bloch oscillation period) for all of the selected BSSLs.

Figure 2 shows the optimized BSSLs we have obtained for different THz frequencies ranging from 1 to 4 THz. The optimized bias field (F), well width (w) and barrier width (b) are shown in the red curves in Figs. 2(a)–2(c). We note that the selected BSSLs represent maxima of the terahertz gain with respect to F, w, and b. To gain some insight into how fast the gain coefficient decreases as F and w are moved away from the maximum, in Fig. 2(a) and 2(b), we use the unshaded regions to indicate the parameter space where the gain coefficient is reduced by less than 30% from the optimal value. The boundaries are obtained by fitting the gain coefficient as a function of one variable, while keeping the other two constants. For instance, at $f=2$ THz, the upper and lower boundaries of F are calculated by fitting the gain coefficient as a function of F, while keeping $w=88$ Å and $b=12$ Å. We note because the values of b are very close to the lower limit set in our simulations (10 Å), its upper and lower boundaries are not calculated.

It can be seen from Fig. 2 that for F, the white region is very narrow, which means that the gain coefficient is sensitive to the bias field. On the other hand, the white region for w is relatively large, thereby allowing a larger variation in w before the gain coefficient is reduced significantly. Figure 2 also shows that the bias field, F, is almost linearly dependent on the central frequency of the THz field. This is perhaps expected because (in the absence of excitonic effects) the WSL spacing is given by eFd and the optimized d is decreasing almost linearly with the THz frequency [Figs. 2(b) and 2(c)]. The well

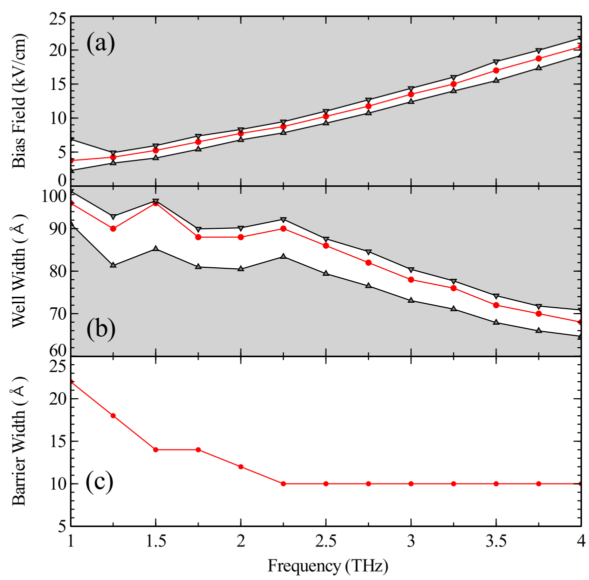

FIG. 2. The (a) bias field, (b) well width, and (c) barrier width for the optimized BSSL structures as a function of the THz frequency. The red lines with filled circles are the optimized values, while the black lines with filled triangles indicate the limits of the range over which the gain is reduced by less than 30%. The results are for $\hbar\Gamma = 0.5$ meV.

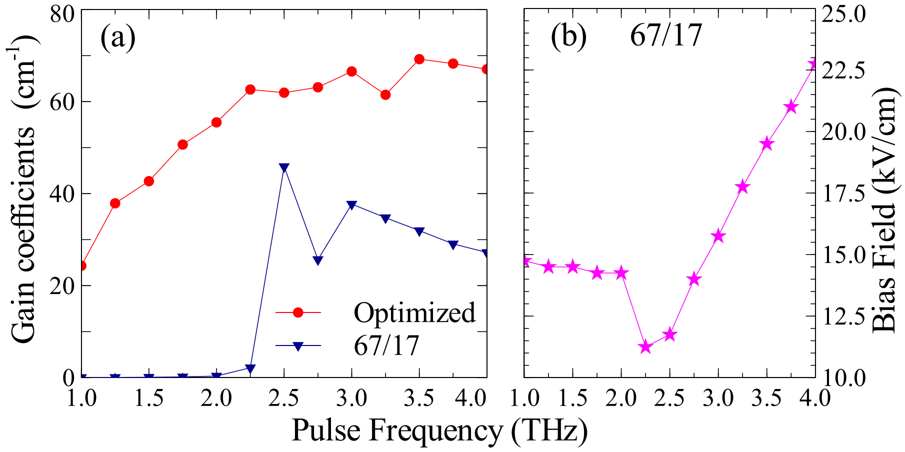

FIG. 3. (a) Gain coefficient of the optimized BSSLs as a function of the THz frequency to be amplified for an exciton density of $N = 1.0 \times 10^{15}/\text{cm}^3$. The red curve with solid circles is for the globally optimized structures given in 2. The blue curve with solid triangles is for a fixed BSSL with $b = 17$ Å and $w = 67$ Å, in which only the bias field is optimized at each frequency. (b) The optimized bias field for the 67/17 BSSL as a function of THz frequency.

width, w, of the best BSSLs is in the range of 68 Å to 96 Å, with the value decreasing with f when $f > 2.25$ THz. Similarly, the barrier width, b, also decreases with the f and becomes a constant at $f = 2.25$ THz where it hits the lower limit we set for allowable b. From the results shown in Fig. 2, we conclude that, to obtain an optimized BSSL, both the well width and the barrier width should decrease as the central frequency of the terahertz field increases. Figure 2 also indicates that using a single BSSL for frequencies ranging from 1 THz to 4 THz is not a good strategy. For example, if we select the structure that is optimized for the frequency of 1 THz ($b = 22$ Å and $w = 96$ Å), its gain coefficient at 4 THz (at the optimized bias field, $F = 17.75$ kV/cm (Ref. 39)) is about 30 times smaller than that of the optimized structure ($F = 20.5$ THz, $b = 10$ Å and $w = 68$ Å, also see Fig. 3).

Having found the optimal BSSLs for each THz frequency value, we now plot the gain coefficients of these structures in Fig. 3. In the calculation, we have used an exciton density of $N = 1.0 \times 10^{15}/\text{cm}^3$, which is relatively low so as to minimize exciton-exciton interactions and is consistent with our previous work.[15] Figure 3 shows that the gain coefficient, for the central frequency f ranging between 1 and 4 THz generally increases with f. For $f \leq 2.25$ THz, the increase is approximately linear; to some extent, this linear dependence arises because $\gamma(\omega)$ is directly proportional to ω. However, for $f > 2.25$ THz, the increase is much slower. The cause of the reduced rate of increase can be seen in Fig. 2(c), where it is seen that no optimization of b was possible when $f > 2.25$ THz as the smallest allowed b had been reached. Therefore the chosen BSSLs for $f > 2.25$ may not be the globally best ones, but one would have to perform calculations beyond the envelope function approximation to obtain reliable results beyond the 10 Å limit, and this would be prohibitively computationally expensive.[37] Finally, we note that the gain coefficients shown here are comparable to those reported with THz quantum cascade lasers.[15,40,41]

The gain coefficient obtained from the optimal BSSLs can be substantially larger than those obtained using a single BSSL. For instance, we investigated a particular BSSL structure with $w = 67$ Å and $b = 17$ Å that has been used in previous[15,28,34,42] For this structure, we followed the procedure described earlier and calculated its properties for different F ranging between 0 kV/cm and 30 kV/cm, resulting in a total of 76 data sets after the initial screening. Then for each given frequency f, we find the optimal bias field F and the corresponding gain coefficient, which are also shown in Fig. 3 for an exciton density of $N = 1.0 \times 10^{15}/\text{cm}^3$. The gain coefficient is no longer linear with f, but shows a peak close to $f \simeq 2.5$ terahertz and a decrease beyond that the obtained gain coefficients are seen to be well below those of the globally optimized structures, but shows reasonable tunability for frequencies greater than 2.5 THz. In addition, the gain coefficient below $f \simeq 2.25$ THz is close to zero because the bias fields required for larger gain ($\sim$5 kV/cm) do not satisfy our initial screening conditions (and thus removed) since the excitonic WSL energy structure is not well established at such low bias fields. Such a situation is also shown in Fig. 1 (although it is a different structure), where at $F = 5$ kV/cm, the condition $(|Q_{-1}|^2 + |Q_0|^2 + |Q_1|^2)/\sum_n Q_n^2 > 0.4$ is not satisfied.

Finally, we briefly discuss the optimal BSSL for $f = 2$ THz, which has the optimal results of $F = 7.75$ kV/cm, $w = 88$ Å and $b = 12$ Å. Figure 1 shows the basic properties of the WSL levels of this structure. The variation of the energy, E_n, of each WSL level with respect to the bias field is shown and the asymmetry in the energy levels can be clearly seen, for instance, $E_0 - E_{-1} < E_1 - E_0$ as $E_0 - E_{-1} = 8.33$ meV and $E_1 - E_0 = 6.87$ meV. As we can see, the $n = -2$, -1, and 1 WSL levels have the largest optical dipole elements, not the $n = 0$ state, which is optically pumped in our simulation. However, this is not critical because the intensity of the pumping laser can be increased to achieve the desired exciton density.

In summary, we have found the optimum optically pumped GaAs/$Al_{0.3}Ga_{0.7}As$ BSSLs to achieve amplification in the THz frequency regime. The optimization process is based on a tight-binding model of BSSLs that includes electron-hole interactions. This computationally efficient model enables us to compute and compare the THz gain of a lager number of different BSSLs. We found that the bias field depends almost linearly on the THz frequency and the well width and the barrier width should decrease as the THz frequency increases for optimal amplification. We believe that this will be useful in designing the first experiments to observe gain in BSSLs which will hopefully pave the way to the design of THz amplifiers.

This work was supported by the National Natural Science Foundation of China under Grant No. 51390472. L.L. acknowledges support from the Department of

Education of Shaanxi Province under Grant No. 2013JK0626 and Xi'an University of Posts and Telecommunications's funding for young faculty members under Grant No. 1050413. M.M.D. acknowledges support from the Natural Sciences and Engineering Research Council of Canada.

[1]D. Clery, Science **297**, 761 (2002).
[2]D. Dragoman and M. Dragoman, Prog. Quant. Electron. **28**, 1 (2004).
[3]R. A. Kaindl, M. A. Carnahan, D. Hagele, R. Lovenich, and D. S. Chemla, Nature **423**, 734 (2003).
[4]T. Suzuki and R. Shimano, Phys. Rev. Lett. **103**, 057401 (2009).
[5]T. Suzuki and R. Shimano, Phys. Rev. Lett. **109**, 046402 (2012).
[6]Z. Zhou, D. Zhang, Z. Zhao, and J. Yuan, Phys. Rev. A **79**, 063413 (2009).
[7]D. Wang, X. Lei, and Z. Wu, J. Phys. Condens. Matter **23**, 345801 (2011).
[8]N. Maeshima and K. Hino, Phys. Rev. B **85**, 205305 (2012).
[9]P. G. Savvidis, B. Kolasa, G. Lee, and S. J. Allen, Phys. Rev. Lett. **92**, 196802 (2004).
[10]T. Ihara, J. R. Cardenas, Y. Sakasegawa, R. Ferreira, G. Bastard, and K. Hirakawa, Phys. Rev. B **86**, 161305 (2012).
[11]B. A. Knyazev, G. N. Kulipanov, and N. A. Vinokurov, Meas. Sci. Technol. **21**, 054017 (2010).
[12]J. Xu, J. M. Hensley, D. B. Fenner, R. P. Green, L. Mahler, A. Tredicucci, M. G. Allen, F. Beltram, H. E. Beere, and D. A. Ritchie, Appl. Phys. Lett. **91**, 121104 (2007).
[13]M. Kress, T. Löff ler, S. Eden, M. Thomson, and H. G. Roskos, Opt. Lett. **29**, 1120 (2004).
[14]V. I. Sankin, A. V. Andrianov, A. O. Zakhar, and A. G. Petrov, Appl. Phys. Lett. **100**, 111109 (2012).
[15]D. Wang, A. Zhang, L. Yang, and M. M. Dignam, Phys. Rev. B **77**, 115307 (2008).
[16]K. F. Renk, A. Rogl, and B. I. Stahl, J. Lumin **125**, 252 (2007).
[17]K. F. Renk and B. I. Stahl, Phys. Lett. A **375**, 2644 (2011).
[18]A. A. Andronov, E. P. Dodin, D. I. Zinchenko, Yu. N. Nozdrin, A. A. Marmalyuk, and A. A. Padalitsa, Quantum Electron. **40**, 400 (2010).
[19]T. Hyart, J. Mattas, and K. N. Alekseev, Phys. Rev. Lett. **103**, 117401 (2009).
[20]G. H. Wannier, Phys. Rev. **117**, 432 (1960).
[21]R. Ferreira and G. Bastard, Surf. Sci. **229**, 424 (1990).
[22]Y. Shimada, K. Hirakawa, M. Odnoblioudov, and K. A. Chao, Phys. Rev. Lett. **90**, 046806 (2003).
[23]A. Ignatov and Y. Romanov, Phys. Status Solidi B **73**, 327 (1976).
[24]A. Lisauskas, M. M. Dignam, N. V. Demarina, E. Mohler, and H. G. Roskos, Appl. Phys. Lett. **93**, 021122 (2008).
[25]H. Willenberg, G. H. Döhler, and J. Faist, Phys. Rev. B **67**, 085315 (2003).
[26]K. Unterrainer, B. J. Deay, M. C. Wanke, S. J. Allen, D. Leonard, G. Medeiros-Riberio, U. Bhattacharya, and M. J. W. Rodwell, Phys. Rev. Lett. **76**, 2973 (1996).
[27]N. Sekine and K. Hirakawa, Phys. Rev. Lett. **94**, 057408 (2005).
[28]A. Zhang, D. Wang, and M. M. Dignam, Appl. Phys. Lett. **86**, 171110 (2005).
[29]Y. Nemoto, K. Hino, and N. Maeshima, Phys. Rev. B **87**, 205305 (2013).
[30]M. Li and X. Mi, Commun. Theor. Phys. **52**, 1134 (2009).
[31]Yu. A. Tarakanov, M. A. Odnoblyudov, K. A. Chao, N. Sekine, and K. Hirakawa, Phys. Rev. B **74**, 125321 (2006).
[32]Y. Li, B. Rosam, and M. Dignam, Phys. Rev. B **72**, 115313 (2005).
[33]The material parameters used in our simulations can be found in Ref. 34.
[34]M. M. Dignam and J. Sipe, Phys. Rev. B **41**, 2865 (1991).
[35]N. Maeshima and K. I. Hino, Comput. Phys. Commun. **183**, 8 (2012).
[36]R. W. Boyd, *Nonlinear Optics* (Academic Press, Burlington, 2008).
[37]We set 10 Å as the lower limit for both layers because the envelope function approximation has reduced accuracy below that size.
[38]F. T. Vasko, Phys. Rev. B **69**, 205309 (2004).
[39]Given the BSSL structure ($w = 96$ and $b = 12$ Å), there are a total of 121 data sets for different bias fields. Because the number is small, we did not apply the initial screening, but worked with all the data.
[40]C. Jirauschek, Appl. Phys. Lett. **96**, 011103 (2010).
[41]Y. W. Huang, W. T. Chen, P. C. Wu, V. A. Fedotov, N. I. Zheludev, and D. P. Tsai, Sci. Rep. **3**, 1237 (2013).
[42]M. M. Dignam and M. Hawton, Phys. Rev. B **67**, 035329 (2003).